TRENDS IN RADAR COUNTS OF MARBLED MURRELETS *BRACHYRAMPHUS MARMORATUS* IN BRITISH COLUMBIA (1996–2018): EFFECTS OF 'THE BLOB' MARINE HEATWAVE AND PREY FISH ABUNDANCE

MARK C. DREVER[1*], MURDOCH K. MCALLISTER[2], DOUGLAS F. BERTRAM[3], BERNARD K. SCHROEDER[4] & KERRY J. WOO[1]

[1]*Environment and Climate Change Canada, Pacific Wildlife Research Centre, 5421 Robertson Road, Delta, British Columbia V4K 3N2, Canada* [*]*(mark.drever@canada.ca)*
[2]*Institute for the Oceans and Fisheries, University of British Columbia, Vancouver, British Columbia V6T 1Z4, Canada*
[3]*Wildlife Research Division, Institute of Ocean Sciences, Environment and Climate Change Canada, Sidney, British Columbia V8L 4B2, Canada*
[4]*Bernard K. Schroeder Consulting, Nanaimo, British Columbia V9R 3R8, Canada*

Received 17 April 2020, accepted 09 October 2020

ABSTRACT

DREVER, M.C., MCALLISTER, M.K., BERTRAM, D.F., SCHROEDER, B.K. & WOO, K.J. 2021. Trends in radar counts of Marbled Murrelets *Brachyramphus marmoratus* in British Columbia (1996–2018): Effects of 'The Blob' marine heatwave and prey fish abundance. *Marine Ornithology* 49: 37–49.

During 2014–2016, the northeast Pacific Ocean experienced a large-scale marine heatwave (nicknamed 'The Blob'), an event that was associated with die-offs of several marine bird species. The Marbled Murrelet *Brachyramphus marmoratus* is a small seabird in this region for which we evaluated trends in abundance—for the purposes of conservation planning—during radar surveys at 58 sites in coastal British Columbia, from 1996 to 2018, and for which we determined whether trends may have been affected by 'The Blob'. A hierarchical Bayesian model allowed us to separate long-term trends from short-term annual fluctuations ('year effects') that might have resulted from changes in ocean conditions, and it also allowed us to test whether predicted regional counts were associated with two indices of marine conditions: (1) measured abundance of a prey species, Pacific Herring *Clupea pallasii*; and (2) sea surface temperature (SST). Province-wide mean annual rate of change in counts was significantly negative, with a posterior median of -0.023 (95% credible interval: -0.033, -0.014); mean rate of change in counts per year was negative for all six Marbled Murrelet Conservation Regions; and trends were significantly negative at the Central Mainland Coast, East Vancouver Island, Haida Gwaii, and the South Mainland Coast conservation regions. Year effects during or after 'The Blob' at West and North Vancouver Island (2016) and East Vancouver Island (2018) conservation regions were not statistically significant. Mean predicted regional counts of murrelets showed weakly positive correlations with age two herring recruitment, and no consistent associations with SST. These results indicate that the marine heatwave did not strongly affect forest-bound murrelets and are consistent with the hypothesis that ongoing loss of terrestrial nesting habitat is associated with population declines of Marbled Murrelets in British Columbia.

Key words: *Brachyramphus marmoratus*, radar counts, marine heatwave, Pacific Herring, sea surface temperature, trends

INTRODUCTION

Similar to heatwaves on land, marine heatwaves periodically occur when large areas of ocean are subject to enduring positive sea surface temperature (SST) anomalies (Oliver *et al*. 2018). Such events are associated with reduced ocean productivity and negative consequences for invertebrates, fish, and bird populations (Frölicher & Laufkötter 2018). During 2014–2016, the northeast Pacific Ocean experienced 'The Blob', the largest marine heatwave recorded to date (Bond *et al*. 2015, Di Lorenzo & Mantua 2016), during which several die-offs of marine birds occurred, including Cassin's Auklet *Ptychoramphus aleuticus*, Common Murre *Uria aalge*, Tufted Puffin *Fratercula cirrhata*, and Red Phalarope *Phalaropus fulicarius* (Gibble *et al*. 2018, Jones *et al.* 2018, Drever *et al.* 2018, Jones *et al.* 2019, Piatt *et al*. 2020). Given that such heatwaves may become more frequent under continued anthropogenic climate warming (Oliver *et al*. 2018), a better mechanistic understanding is needed of how such events affect the population dynamics of marine birds.

The Marbled Murrelet *Brachyramphus marmoratus* is a small marine bird whose breeding range extends from California to Alaska; it is listed as Threatened, both in Canada under the *Species at Risk Act*, and in the United States under the *Endangered Species Act* for California, Oregon, and Washington states, due to ongoing declines throughout its southern range. The primary conservation concerns are loss of old growth forest nesting habitats and marine threats, including oil pollution, marine vessel traffic, mortality from gillnet entanglement, and ocean climate anomalies that affect food webs (COSEWIC 2012). Changes in ocean conditions, such as those that result from marine heatwaves, can result in large-scale year-specific shifts in the abundance and distribution of Marbled Murrelets (Bertram *et al*. 2015). In 2005, large reductions in the number of murrelets were observed along the west coast of Vancouver Island relative to 2004 and 2006, when ocean conditions facilitated a greater availability of fish prey (Ronconi & Burger 2008). In Washington State, counts of Marbled Murrelets from 1995 to 2012 indicated a correlation between Marbled Murrelet density and indices of El Niño Southern Oscillation (ENSO), which was thought to occur, in part, due to movements of murrelets from other areas during poor years on the outer coast (Lorenz & Raphael 2018). Ocean conditions appear to be a key driver of short-term occupancy dynamics of Marbled Murrelets throughout much of the Oregon coast (Betts *et al*. 2020). Therefore, when considering the role of ocean conditions on the population viability of Marbled Murrelets, these temporary effects can be distinguished from long-term trends as 'year effects,' that is, year-specific deviations in murrelet counts away from the long-term trajectory in abundance. Furthermore, given the spatial variability that can occur in ocean conditions, differentiating year-specific deviations from long-term trends will need to be region-specific (Bertram *et al*. 2015), precipitating the need for novel statistical approaches to estimate long-term trends across large landscapes.

In this paper, we update the trend estimates presented in Bertram *et al.* (2015) of Marbled Murrelet abundance based on radar counts for the entire coast of British Columbia, Canada, including 56 additional surveys during 2014–2018, a period of time that included 'The Blob'. The statistical model applied extends the one presented in Bertram *et al*. (2015), which accounts for the spatial structure of the survey design and for potential differences in trends between different conservation regions. The chief objective of the analysis was to update province-wide trends of Marbled Murrelets, extending the period for an additional five years to cover 1996 to 2018, using a hierarchical Bayesian model of radar counts (Bertram *et al*. 2015). This model included terms to account for spatial variance in trends, seasonal variance in counts (day of year, DOY), and effects of radar tilt, which allowed us to evaluate yearly deviations ('year effects') from mean trends. In addition, we tested whether average region-wide counts were correlated with ocean conditions and prey abundance, as measured by sea surface temperature (SST) and estimates of age two recruitment for Pacific Herring *Clupea pallasi*, an important prey of Marbled Murrelets (Burkett 1995), respectively. Unlike Pacific Sand Lance *Ammodytes hexapterus*, which is another important prey of Marbled Murrelets, Pacific Herring abundance is assessed annually at each Marbled Murrelet conservation region. We predicted that if the marine heatwave affected trends in murrelet abundance, year effects during or after the heatwave would be significantly negative and that murrelet counts would be negatively associated with SST. Alternatively, we predicted that if murrelet counts were related to annual fluctuations in prey fish, we would observe a positive correlation between counts and estimates of herring recruitment.

METHODS

Study sites and radar counts

Counts of Marbled Murrelets were conducted from 1996 to 2018 at sampling stations distributed within six Marbled Murrelet conservation regions in British Columbia, as determined by the Canadian Marbled Murrelet Recovery Team (Fig. 1). Raw data of Marbled Murrelet counts are available on the website (Appendix 1). Radar count protocols are provided in Manley (2006) and Bertram *et al.* (2015) and are only briefly described here. Within a year, each radar station was surveyed three times, from early May to mid-August, with two surveys on consecutive days and the third on a non-consecutive day. Surveys were conducted at radar stations in the hours before dawn, during which each target was identified on radar screens as a murrelet based on their size and speed, and tallied as in-bound or out-bound depending on their trajectory. Weather conditions were recorded at the beginning and throughout the survey period. Most stations were only accessible by vessel and, hence, were 'boat-based' stations (except for Nitinat, Toquart, and Tahsis in the West and North Vancouver Island Conservation Region, which could also be accessed by vehicle), in contrast to stations on East Coast Vancouver Island which were accessible by

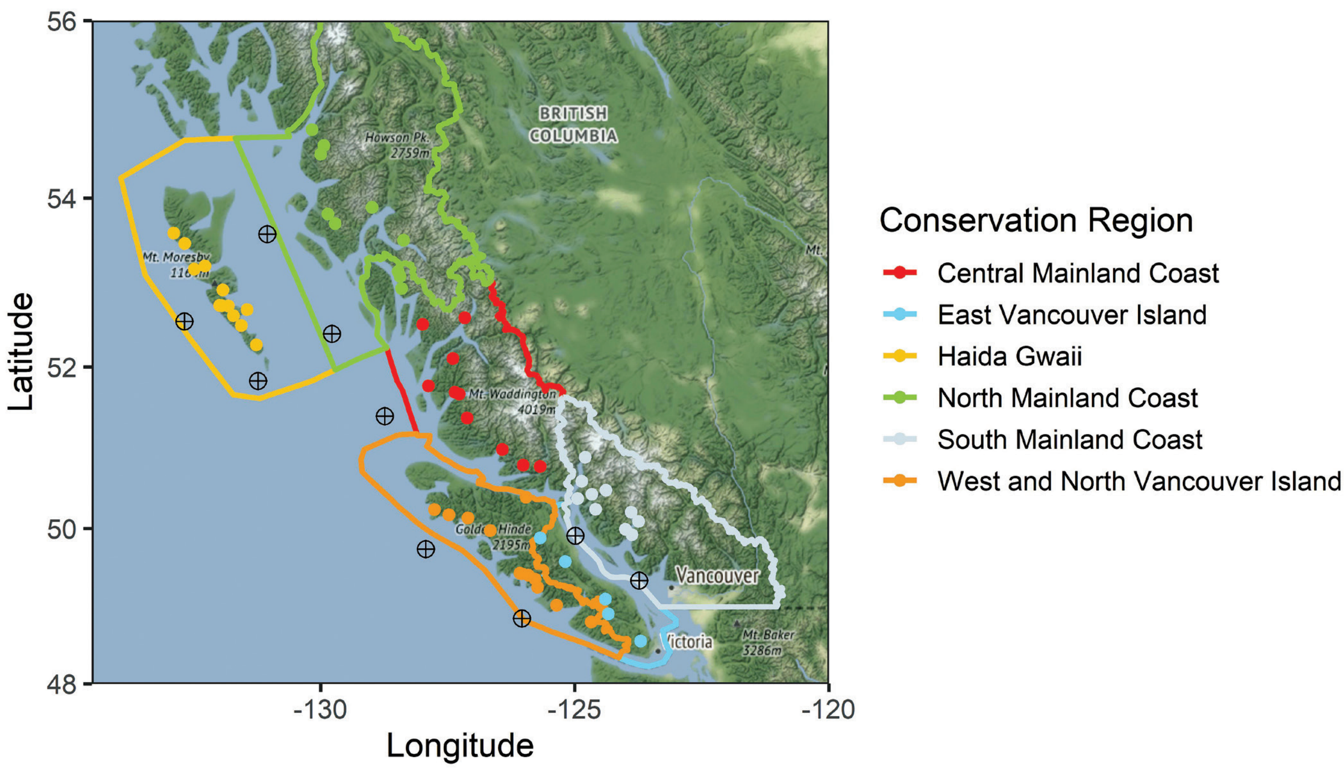

Fig. 1. Locations of long-term radar monitoring stations maintained by Environment and Climate Change Canada in six conservation regions of British Columbia, Canada. Colour points indicate locations of individual stations. Black-cross points indicate locations of marine buoys from which information on sea surface temperature was obtained. A more detailed version of this map is provided in Bertram *et al.* (2015).

truck. A total of 1 014 radar counts were conducted from the same 58 sites as in Bertram *et al.* (2015).

Statistical model

We modified the hierarchical Bayesian model from Bertram *et al.* (2015) in the following ways. First, we re-evaluated the year effects model component with the updated time series to 2018 to test whether additional year effects could be included. Second, to provide a more parsimonious characterization of seasonal trends, we adjusted the prior for the parameter determining whether there was one or two peaks in counts within each year. Third, we assumed that the shape parameter describing how the expected radar count varied with DOY was the same across regions (see below for details). Fourth, we replaced the lognormal likelihood function with a negative binomial likelihood function (Hilborn & Mangel 1997) to allow for overdispersion in the count data and zero counts to be included without assigning one's to the zero counts. Fifth, we placed bounds on factors related to the linear count trend component and common shared year effects to prevent the product of two negative values from producing a large positive predicted count. Sixth, because we needed a time series of counts by region for each sampled year to test for correlations between counts and indices of ocean conditions, we developed a new model prediction to formulate region-specific average counts by sample year.

General form of statistical model of radar count at each site in each year

The general form of the model to predict the radar count at each site in each year from Bertram *et al.* (2015) is given by:

$$C_{p,s,i} = (b_{o,s} + b_{1,s} \times (y_{s,i} - \bar{y}_s)) \times (1 + \tau_R|y_{s,i}) \times (1 + a_R\,(D_i - c_R\,)^2) \times (1 + t \times T_i) \quad (1)$$

where $b_{o,s}$ and $b_{1,s}$ are the coefficients for the average radar count and year covariate in each site s, $\tau_R|y_{s,i}$ is the year effect for year $y_{s,i}$ common to all sites in region R, a_R is the region-specific coefficient for the rate of change in detection from the mid-year point, D_i is the DOY with 182 subtracted so that the covariate is centered at zero at the mid-point of the year, c_R is the region-specific coefficient for the deviation from the mid-year point, where the detection rate is either maximum (or at a minimum, depending on the sign of a_R), and t is the coefficient for the radar tilt covariate T_i.

At the core of the estimation is a slope parameter (b_1) term that describes the average change in counts per year for a given station. The abundance intercept term (b_o) for each site was referenced to the mean year for each site. In the reference case model, both b_1 and b_o were treated as exchangeable across the 58 sites.

$$b_1 \sim \text{Normal } (\mu_{b1}, \sigma^2_{b1}) \text{ (2a)}$$

$$b_o \sim \text{Normal } (\mu_{bo}, \sigma^2_{bo}) \text{ (2b)}$$

where the terms in the parentheses are the hyperparameters that were estimated within the hierarchical model. Fixed priors were placed on each of the hyperparameters in equations 2a and 2b. These were vague in shape and with either normal, uniform, or lognormal form depending on whether the parameters were restricted to be non-negative or not. Specifications for the priors for all of the parameters are listed in Table 1. We considered various model formulations prior to settling on this model, and we settled on this version as a parsimonious model that best accounted for year effects common to all sites within a region and the effect of radar tilt, and the DOY for each radar count (for full details, see McAllister 2019).

Estimation of trends in abundance

As a measure of trend, we used the estimated rate of change over time calculated as slope/intercept (b_1/b_0 =rate), where the intercept b_0 is referenced to the expected count in the mean year for each site. This measure standardizes the trend by the average abundance at

TABLE 1
Prior distributions for key parameters in trend model used to predict radar counts for Marbled Murrelets *Brachyramphus marmoratus* in British Columbia, Canada

Parameter	Definition	Distribution	1st Parameter[a]	2nd Parameter[a]
μ_{bo}	Hyper parameter for mean of intercepts	Uniform	1	2000
σ_{bo}	Hyper parameter for standard deviation of intercepts	Log-normal	3.91	1.5625
μ_{b1}	Hyper parameter for mean of slopes	Normal	0	0.0001
σ^2_{b1}	Hyper parameter for standard deviation of slopes	Log-normal	2.30	1.5625
$b_{o,s}$	Mean count for site	Log-normal	μ_{bo}	σ_{bo}
$b_{1,s}$	Slope for site	Normal	μ_{b1}	σ^2_{b1}
σ_Y	Hyper parameter for standard deviation of year effects	Log-normal	2.303	1.5625
$Y_{R,y}$	Year effect	Normal	0	σ_Y
a	Day of year effect – coefficient a	Normal	0	10000
c_R	Day of year effect – coefficient c for each region R	Normal	0	0.01
t	Radar tilt coefficient	Normal	0	1

[a] For the normal distribution, the 1st parameter is the mean and the 2nd parameter is the precision (1/variance). For the gamma distribution, these are α and β. For the uniform distribution, these are the lower and upper bounds. For the lognormal distribution, the 1st parameter is the natural logarithm of the median, and the 2nd parameter is the precision in the natural logarithm of the random variable.

each site and thus makes the rates directly comparable. Further, for conservation regions where year effects have been estimated (see below), it separates the overall trend in the series from the yearly region-wide fluctuations and may better capture the underlying temporal tendency in the counts. The probability of decline, *P* (decline), for each site was computed as the proportion of Markov Chain Monte Carlo (MCMC) runs in which the rate parameter was negative, and was averaged by region or coast-wide to derive estimates as larger spatial scales.

Statistical formulation for year effects

For each conservation region, sets of years were identified as candidates for which common shared year effects were to be estimated. Year effects were considered to be the same across sites by year within a region and could only be estimated in years where year effect estimates were not confounded with site-specific slope and intercept terms. This was typically possible for years in which radar counts were taken at four or more stations. The prior standard deviation for each year effect term was set to be the same across all regions and years. The variance in year effect terms was thus considered to be constant across sites and between regions. The prior mean for year effects was held at zero. The prior density function for the standard deviation in year effects, σ_τ, was given by:

$$\sigma_\tau \sim \text{LogNormal}\,(\mu_{\sigma_\tau}, \sigma^2_{\sigma_\tau}) \quad (3)$$

where the terms inside of the parentheses are the prior mean and prior variance in σ_τ, which were both estimated. σ_τ was assumed to be the same between the different regions. Based on inspection of cross-site sampling by year for sites within each region, year effects were set to zero for years for which it was judged that confounding would occur between year effect coefficients and the slope and intercept coefficient for each site. For example, if a number of sites had only three years where radar counts were taken, no year effect was estimated. However, if there were a number of other sites where these same years were sampled in addition to other years, then one trial year effect was sampled.

We applied some additional criteria to determine which year effects to estimate within each region. For example, where there were several years in common between sites within a region, the year effect that was set to zero was that which was common to all sites and was one of the central years surveyed within the region. This reduced the possibility of confounding in estimates of year effects and slope within each region.

Accounting for day of year effects

To accommodate for seasonal changes in abundance, where maximum radar counts tended to occur around the middle of the year, a second order polynomial function of the DOY was adopted that included coefficient *a* for the curvature of the parabola (i.e., the rate at which counts decay as one goes further away from the DOY with the maximum expected counts). A second coefficient *c* characterized the deviation from the mid-year point at which maximum counts occur (i.e., the number of days away from 30 June that the maximum counts tend to occur in a given region). We modified the priors from those applied in Bertram *et al.* (2015). The prior for parameter *a* was modified to be uniform between -0.02 and zero, thereby excluding the possibility of positive values, and was assumed to be the same across the different regions. There was no clear empirical support for more than a single seasonal peak in counts. For the fewer than five of the 58 monitoring stations where either one or two peaks could be fit, the model selection criterion, i.e., the Deviance Information Criterion (DIC), was not significantly different when comparing a model with one versus two peaks. All of the remaining stations had a distinct single seasonal peak in counts. The Bertram *et al.* (2015) model was over-parameterized when unique shape parameters for seasonal pattern in counts were fitted for each of the 58 stations, as evidenced by very little update in estimates of parameters used to predict seasonal patterns within a site. The parameter *a*, which determined the gradient in seasonal count with DOY, was very poorly determined on a site-by-site and region-by-region basis. It was reasonably well-determined only when a single shape parameter *a* was estimated for all six regions. The average DOY for the peak count was well-determined when fitted for each region and was found to differ significantly between regions, so we could only justify fitting a peak average DOY for counts by region, but not at a finer resolution, such as by station. The prior for parameter *c* was modified to allow for larger deviations from the prior mean. It had a normal distribution, with a prior mean for *c* of zero and the prior standard deviation in *c* increased to 30.

Accounting for the tilt angle of the radar

As in Bertram *et al.* (2015), radar tilt was modelled as a covariate. This covariate had a normal prior distribution with a mean of zero and standard deviation of one.

Likelihood function of the radar count data

Given that nearly all of the counts were within two orders of magnitude of each other, the frequency distribution of counts for different sites showed a positive skew, and there were very few zero observations (< 1% of all observations), a lognormal probability model of the data (i.e., likelihood function) was applied in Bertram *et al.* (2015). However, given that the incidence of zero counts persisted across years and sites, and tended to become more frequent in the later years of the time series, the lognormal density function was replaced with a negative binomial probability model that could directly model the zero counts. We used the formulation from Hilborn & Mangel (1997), which is parameterized based on the expected mean count (i.e., $c_{p,s}$ from Equation 1) and an overdispersion parameter *k*, (i.e., the smaller the value for *k*, the larger the overdispersion in the counts). The probability that the observed count on a given site *s* is the one realized ($C_{o,s} = c_{o,s}$) (ignoring subscripts year (y), observation within year (i)) is given by:

$$P\left(C_{o,s} = c_{o,s}\right) = \frac{(k_s + c_{o,s})}{(k_s)\, c_{o,s}!} \left(\frac{c_{p,s}}{k_s + c_{p,s}}\right)^{c_{o,s}} \left(1 + \frac{c_{p,s}}{k_s}\right)^{-k_s} \quad (4)$$

where k_s is the overdispersion parameter for site *s* and $c_{p,s}$ is the predicted count for site *s* (Equation 1). It was not possible to estimate k_s for each site simultaneously with the other estimated parameters in a single WinBUGS model run. Therefore, the overdispersion factor k_s was estimated for each site using an iterative approach. An initial vector of fixed values for k_s by site was applied in the first WinBUGS estimation. The resulting posterior median predicted values for each observed radar count for each site was then applied outside of the WinBUGS estimation to find the best fitting value of *k* for each site in a function minimization that fitted the above negative binomial model to the posterior median outputs for radar counts for each of the sites. Four sets of WinBUGS model runs were carried out to arrive at a final set of values for k for each site.

Diagnostics applied

WinBUGS 1.4.3 statistical software was used for our analysis (http://www.mrc-bsu.cam.ac.uk/bugs). Several diagnostics were computed to identify models that could explain the data (Appendix 2, available on the website) and were not over-parameterized. Trace plots were monitored for key variables to ensure that the parameter values in different chains were mixing and following a stable trajectory within each model run. Autocorrelation in values simulated within Markov Chains was computed and inspected for each estimated parameter to evaluate the degree of autocorrelation between parameters within the Markov chains at different lags within the chains. Posterior correlations between estimated parameters were computed and inspected for the presence of a high degree of correlation between estimated parameters. In the model selected, the posterior correlations that were checked were not large in magnitude for the pairs of parameters inspected (i.e., they were all less than 0.6 in magnitude).

The Gelman-Rubin statistic was monitored for all estimated parameters to identify the burn-in for each MCMC run and to ensure that following the burn-in, the parameter values in the different chains were mixing and conforming to a stabilized target distribution. Marginal posteriors for key parameters were inspected for evidence of indeterminance (i.e., lack of update in the prior due to insufficient or uninformative data to enable sufficiently precise estimation). When posteriors for a given trial parameter were very similar to the prior, the trial parameter was removed. If there were two or more pronounced modes in the posterior distribution for a given parameter, it was concluded that the available data did not permit reliable estimation of all model parameters over the range of values specified in their priors. Either (i) the parameter itself was eliminated from the model structure, (ii) the prior for the parameter was inspected and, if appropriate, it was modified to restrict its range, or (iii) one or more common year effect coefficients that caused the confounding were eliminated.

Test for associations between counts and covariates for oceanic conditions

To test for associations between radar counts in each region and covariates for oceanic conditions, we calculated the predicted average count by year, $C_{R,y}$, in a region, that was standardized for tilt effect and DOY effect for each region, such that:

$$C_{R,y} = b_{o,R}\,(1 + r_R \times (y - \bar{y}_R)) \times (1 + \tau_R|y) \times (1 + \alpha(D_R - c_R)^2) \times (1 + t \times T_R) \quad (5)$$

where $b_{o,R}$ is the mean intercept across sites in region R, τ_R is the mean rate of change (slope/intercept) across sites in region R, $\bar{y}_R$ is the mean year in region R, $\tau_R|y$ is the estimated common shared year effect for year y in region R, D_R is the standard DOY for region R, a is the DOY coefficient, c_R is the mean DOY coefficient for region R, t is the tilt coefficient, and T_R is the standard radar tilt applied for region R.

Two different covariates of ocean conditions were considered because they were available in sufficient regional detail to be associated with Marbled Murrelet Conservation Regions. First, we considered mean annual sea surface temperature (SST) by year from National Oceanic and Atmospheric Administration (NOAA) buoys present in oceanic waters within each Marbled Murrelet Conservation Region. SST allowed us to link abundance of murrelets to the underlying consideration of marine heatwaves. We obtained SST data from NOAA buoys distributed throughout the study area (Fig. 1). Where two buoys fell within a region, the mean annual SST was computed. If there was only one annual SST available from the two buoys in a given year, the annual SST was set to the buoy where a SST was available. Second, we considered estimates of age two recruitment for Pacific Herring from the Pacific Herring management area most closely associated with each Marbled Murrelet Conservation Region. Marbled murrelets forage on a variety of prey fish (Burkett 1995), including herring, Pacific Sand Lance, and Northern Anchovy *Engraulis mordax*. A long time series (1952–2018) of age two Pacific Herring abundance, including seven stocks, is available for the Pacific coastal herring fishery management region, which is assessed annually by Fisheries and Oceans Canada. Close correspondence exists between five of the Pacific Herring fishery management areas (Strait of Georgia, West Coast Vancouver Island, Haida Gwaii, Central Coast, Prince Rupert) and the six Marbled Murrelets Conservation Regions. There are no other stocks of forage fish where juvenile abundance is estimated on a regular basis to provide forage fish abundance time series that correspond to the time series of radar counts. Estimates of age two Pacific Herring recruitment for five different Pacific Herring management areas were provided by the Department of Fisheries and Oceans of the Canadian federal government (Appendix 3, available on the website).

To reduce the risk of spurious correlations between Marbled Murrelet counts and the two environmental covariates, which could result from co-occurring time trends in the count and the covariate, the predicted regional counts and environmental covariates were first differenced to formulate the dependent variable and independent variable for correlation analysis. Spurious correlations between two variables can often be found when both time series have experienced systematic time trends. It is common to control for the detection of spurious correlations between different time series by taking the difference between consecutive observations in each time series. Thus, $dY(t) = Y(t) - Y(t\text{-}1)$ and $dX(t) = X(t) - X(t\text{-}1)$, where $Y(t)$ would be the radar count of murrelets in year t, $X(t)$ would be the estimate of age two herring abundance in year t, and $dY(t)$ and $dX(t)$ are the differenced values for X and Y between times t and t-1. Therefore, if there were a causal (e.g., positive) relationship between the two variables, X and Y, then the dependent variable Y would be expected to increase the most between one time step and the next when the independent variable X was observed to have increased the most between those two same time steps, and vice versa. Thus, in the situation in which both time series showed significant trends, differencing both variables and then testing for a correlation between the differenced variables could be expected to show no significant correlation when there was no causal relationship between the two variables. To account for potential lags in effects, each of the environmental indices was lagged by zero, one, or two years. The SST measures were lagged by zero (no lag) and then one year to produce two different sets of SST indices to test. The age two Pacific Herring recruitment data were lagged by either zero (age two at the beginning of the year, weighing about 25–62 g depending on the year), one (age one at the beginning of the year, about 5–10 g), or two years (age zero at the beginning of the year, < 1 g).

Exploratory analyses were carried out by first plotting the differenced murrelet counts and differenced oceanic indices to check whether there were any consistent patterns across the six regions in the relationship between murrelet count and each oceanic index. Where a consistent relationship was found, linear models were fitted to the data to test the null hypothesis that the slope was equal to zero, i.e., that the slope coefficient for herring was less than or equal to zero and the slope coefficient for temperature was larger than or equal to zero.

RESULTS

Our model treated slope, intercept, and year effects as hierarchical; estimated a single DOY coefficient *a* for all regions and *c* coefficients different between regions; estimated 33 year effects; and treated tilt as a covariate. Using data from 1 014 radar surveys, a total of 168 parameters were estimated and the model provided an excellent fit to the wide spatial and temporal variation in radar counts across coastal British Columbia, which varied from less than 10 to over 1 500 birds per survey (Appendix 3). The median of posterior distribution for the hierarchical mean of the slope parameters between sites was negative, and its 95% credibility interval did not overlap with zero (Table 2). The posterior mean and standard deviation for the intercept term (i.e., the average number of counts per site) indicated that more than an order of magnitude of variation existed between sites in the mean radar count (Table 2).

Trends in murrelet abundance

The derived rate (slope/intercept) for each site provided an indication of the average rate of change in radar counts over the time period (Table 3) and indicated a continued decline from 1996 to 2018 (in accord with trends from 1996 to 2013, as in Bertram *et al.* (2015)). The province-wide annual rate of change was significant, with a posterior median of -0.023 (95% credible interval: -0.033, -0.014 (Table 3)). The mean relative change in counts per year was negative for all six conservation regions (Table 3) and was significantly different from zero (at the 5% level) for the Central Mainland Coast, East Vancouver Island, Haida Gwaii, and South Mainland Coast conservation regions (Fig. 2). East Vancouver Island had the most severe negative rate of change, with a posterior median of -0.07 per year, whereas the North Mainland Coast and Central Mainland Coast had the least severe declines, at -0.005 and -0.014% per year. Individual sites with significant negative trends included Kwalate and Koeye in the Central Mainland Coast; Lake Cowichan, and Nanaimo Lakes on East Vancouver Island; no sites on West and North Vancouver Island; Huston and Long on Haida Gwaii; East Inlet on the North Mainland Coast; and Brittain, Deserted, Forbes, Quatam, and Southgate in the South Mainland Coast (Table 3). The slope and rate of change estimates were negative for all of these sites (Table 3). The overall tendency was for the rate of change to be negative, with 51 of 58 sites showing these negative rates. Note that these slope and rate of change coefficients indicated the underlying long-term average trend in counts at each site and accounted for common shared year effects within the region.

Year effects

The posterior mean estimate of the standard deviation in year effects was 0.42, indicating that common year effects could, on average, increase or decrease counts among years away from the underlying trend by ± 50% (Table 2). Time series of estimated common shared year effects were available for East Vancouver Island, West Coast Vancouver Island, and the South Coast conservation regions (Fig. 2). Significant common shared year effects were found in 13 of the 33 years in which these effects were estimated. Twelve were negative and 22 were positive in value (Table 4). Significant common shared year effects were found in the Central Mainland Coast, East Vancouver Island, West and North Vancouver Island,

TABLE 2
Posterior medians, 95% bounds, and medians for key parameters in a hierarchical Bayesian model used to predict radar counts of Marbled Murrelets *Brachyramphus marmoratus* in British Columbia, Canada, 1996–2018

Parameter[a]	Definition	Region[b]	Median	2.50%	97.50%
μ_{bo}	Hyper parameter for mean of intercepts		58.1	44.6	78.5
σ_{bo}	Hyper parameter for standard deviation of intercepts		0.79	0.65	0.99
μ_{b1}	Hyper parameter for mean of slopes		-0.80	-1.46	-0.21
σ_{b1}	Hyper parameter for standard deviation of slopes		1.70	0.93	2.92
σ_Y	Hyper parameter for standard deviation of year effects		0.43	0.30	0.64
a	Day of year effect – coefficient a		-3.2E-04	-3.8E-04	-2.4E-04
c_R [1]	Day of year effect – coefficient c	CC	-4.3	-13.2	6.3
c_R [2]	Day of year effect – coefficient c	EV	3.8	-1.6	10.8
c_R [3]	Day of year effect – coefficient c	WC	12.9	7.6	18.4
c_R [4]	Day of year effect – coefficient c	HG	13.1	5.0	21.6
c_R [5]	Day of year effect – coefficient c	NC	-6.5	-14.4	1.4
c_R [6]	Day of year effect – coefficient c	SC	-3.2	-11.5	5.0
t	Radar tilt coefficient		0.12	0.07	0.17

[a] Number refers to index for each Marbled Murrelet Conservation Region

[b] Region refers to Marbled Murrelet Conservation Regions (Fig. 1), including Central Mainland Coast (CC), East Vancouver Island (EV), West and North Vancouver Island (WC), Haida Gwaii (HG), North Mainland Coast (NC), and South Mainland Coast (SC).

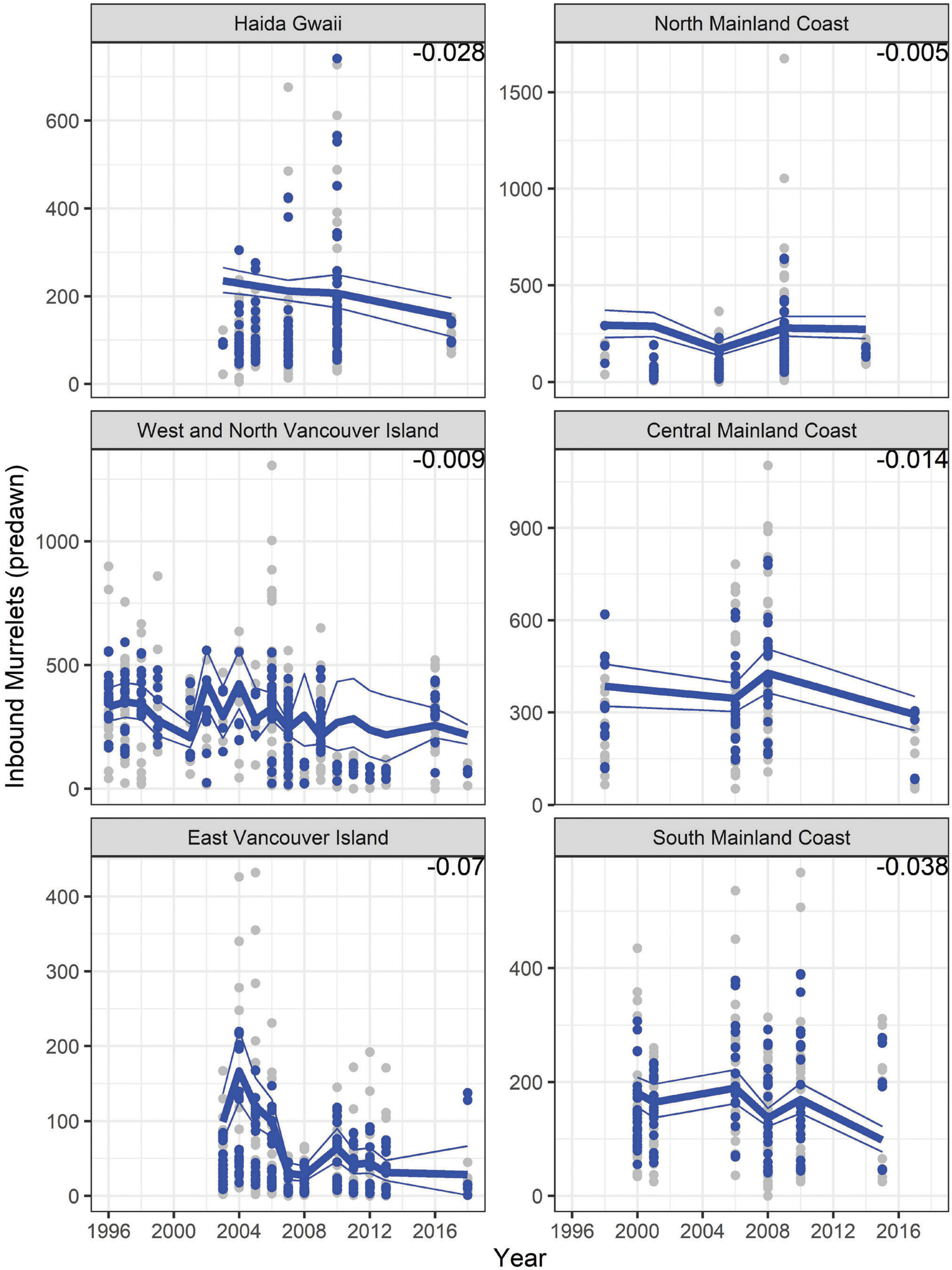

Fig. 2. Temporal trends in the number of Marbled Murrelets *Brachyramphus marmoratus* counted at radar stations distributed through six conservation regions in British Columbia, Canada, 1996–2018. Thick blue lines indicate predicted means from the trend model, with 95% credibility intervals that depict the within-region yearly variation. Blue points indicate the predicted count and grey points indicate the observed counts. The number at the top right of each panel indicates the rate of change for each conservation region.

TABLE 3
Posterior medians for the mean rate of change (i.e., slope/intercept) in abundance of Marbled Murrelets *Brachyramphus marmoratus* for each site, six conservation regions, and coast-wide, as observed in radar counts conducted throughout coastal British Columbia, Canada, 1996–2018[a]

Region/Site	Median	Lower 95% CL	Upper 95% CL	*P* (decline)
Coast-wide	**-0.024**	**-0.033**	**-0.014**	**1.00**
Haida Gwai Conservation Region	**-0.028**	**-0.049**	**-0.010**	**1.00**
Bigsby	-0.018	-0.05	0.02	0.85
Botany	-0.046	-0.12	0.01	0.93
Dawson Inlet	-0.020	-0.08	0.04	0.76
Fairfax	-0.046	-0.15	0.02	0.91
Huston	-0.062	-0.14	0.00	0.97
Hutton	**-0.067**	**-0.13**	**-0.01**	**0.99**
Klunkwoi	0.001	-0.03	0.06	0.47
Lagoon	-0.004	-0.05	0.05	0.56
Long	**-0.033**	**-0.06**	**-0.01**	**0.99**
Port Chanal	-0.002	-0.02	0.01	0.61
Tartu	-0.024	-0.08	0.02	0.85
Windy Bay	-0.015	-0.06	0.02	0.83
North Mainland Coast Conservation Region	-0.005	-0.020	0.013	0.70
Aaltanhash	0.006	-0.05	0.07	0.43
Brim River	0.018	-0.03	0.07	0.26
East Inlet	-0.041	-0.07	-0.01	0.99
Gilttoyees	-0.014	-0.06	0.03	0.74
Green	-0.015	-0.06	0.02	0.82
Khutze	0.011	-0.03	0.06	0.31
Khutzeymateen River	-0.001	-0.03	0.05	0.53
Kwinamass River	-0.002	-0.02	0.02	0.62
Toon River	-0.006	-0.03	0.02	0.72
West and North Vancouver Island Conservation Region	-0.009	-0.019	0.002	0.95
Bedwell	-0.011	-0.03	0.01	0.82
Bulson	-0.013	-0.03	0.01	0.87
Kelsey Bay	-0.001	-0.05	0.06	0.52
Klasksish	-0.014	-0.04	0.01	0.90
Megin	-0.017	-0.03	0.00	0.96
Moyeha	-0.008	-0.03	0.02	0.76
Nitinat	-0.001	-0.03	0.03	0.52
Power	-0.012	-0.04	0.01	0.83
Tahsis	-0.015	-0.04	0.01	0.84
Tahsish	-0.008	-0.03	0.01	0.80
Toquart	-0.010	-0.03	0.02	0.77
Watta	-0.003	-0.03	0.03	0.59

Table 3 continued on next page

Table 3 continued from previous page

Region/Site	Median	Lower 95% CL	Upper 95% CL	*P* (decline)
Central Mainland Coast Conservation Region	**-0.014**	**-0.027**	**-0.001**	**0.98**
Ellerslie	-0.014	-0.04	0.01	0.90
Kakweikan	-0.005	-0.03	0.02	0.67
Kilbella	-0.005	-0.03	0.02	0.68
Koeye	-0.042	-0.07	0.00	0.98
Kwalate	-0.045	-0.10	0.00	0.98
Kwatna	0.001	-0.01	0.02	0.44
Nekite	-0.016	-0.06	0.02	0.82
Skowquiltz	-0.004	-0.05	0.05	0.57
Wakeman	-0.009	-0.05	0.03	0.72
Wannock	-0.004	-0.03	0.03	0.61
East Vancouver Island Conservation Region	**-0.070**	**-0.107**	**-0.034**	**1.00**
Comox Lake	-0.044	-0.10	0.01	0.95
Lake Cowichan	**-0.072**	**-0.11**	**-0.04**	**1.00**
Nanaimo Lakes	**-0.187**	**-0.30**	**-0.09**	**1.00**
Sooke Lake	-0.027	-0.07	0.03	0.83
Upper Campbell	-0.016	-0.06	0.02	0.78
South Mainland Coast Conservation Region	**-0.038**	**-0.054**	**-0.022**	**1.00**
Brem	-0.004	-0.02	0.01	0.68
Brittain	**-0.083**	**-0.13**	**-0.02**	**0.99**
Deserted	**-0.090**	**-0.14**	**-0.04**	**1.00**
Forbes	**-0.072**	**-0.09**	**-0.05**	**1.00**
Orford	0.009	-0.03	0.05	0.32
Quatam	**-0.041**	**-0.07**	**-0.01**	**0.99**
Skwakwa	0.016	-0.03	0.07	0.26
Southgate	**-0.085**	**-0.13**	**-0.03**	**1.00**
Toba	-0.015	-0.04	0.02	0.84
Vancouver	-0.023	-0.08	0.04	0.78

[a] Statistical significance is attributed when the 95% credible interval does not overlap with zero and is shown in bold. Probability of decrease is also shown for each site and across the six regions. Trends coast-wide and for each conservation region represent the mean rate of change for the component sites. CL refers to credibility limit. *P* (decline) refers to the probability of a decrease in counts over time, computed as the proportion of model runs in which the rate parameters for the region/site was negative (see Methods).

the North Mainland Coast, and the South Mainland Coast regions, but not for Haida Gwaii (Table 4). In the West and North Vancouver Island region, the year effect for 2016 was not significant and therefore does not support the hypothesis that the marine heatwave negatively affected counts in the year immediately following the event. Similarly, no significant year effects were found for the South Mainland Coast in 2015 or for the Central Mainland Coast in 2017 (Table 4).

Day of year and tilt effects

The DOY coefficients for five regions (East Vancouver Island, West and North Vancouver Island, Haida Gwaii, North Mainland Coast, South Mainland Coast) showed a maximum count near the mid-point of the year (end of June), with a significant negative estimate for DOY coefficient *a* (Table 2). The deviation from the year mid-point for maximum/minimum counts were significant for East Vancouver Island, West and North Vancouver Island, and Haida Gwaii, with posterior median values of about four, 18, and seven days after the summer solstice (Table 2). The estimates were not significantly different from zero for the Central Mainland Coast, North Mainland Coast, and South Mainland Coast. The posterior estimates for the tilt coefficient were significant and positive, and for a tilt of 12.3°, for example, would give a posterior mean multiplicative effect of about 1.2 (Table 2).

TABLE 4
Posterior 95% bounds and medians for the year-effect coefficients from a hierarchical Bayesian model of temporal trends of Marbled Murrelets *Brachyramphus marmoratus*, as observed in radar counts at six conservation regions in British Columbia, Canada, 1996–2018[a]

Region	Year	2.50%	Median	97.50%
Central Mainland Coast	2008	0.06	0.27	0.52
East Vancouver Island	2003	-0.41	-0.16	0.19
East Vancouver Island	2004	0.08	0.48	1.02
East Vancouver Island	2005	-0.18	0.13	0.53
East Vancouver Island	2007	-0.79	-0.68	-0.51
East Vancouver Island	2008	-0.79	-0.69	-0.53
East Vancouver Island	2010	-0.43	-0.15	0.24
East Vancouver Island	2011	-0.62	-0.39	-0.03
East Vancouver Island	2012	-0.58	-0.30	0.13
East Vancouver Island	2013	-0.68	-0.45	-0.07
East Vancouver Island	2018	-0.37	0.13	0.84
West and North Vancouver Island	1996	-0.01	0.24	0.57
West and North Vancouver Island	1997	0.06	0.32	0.68
West and North Vancouver Island	1998	0.03	0.30	0.65
West and North Vancouver Island	1999	-0.19	0.06	0.39
West and North Vancouver Island	2001	-0.36	-0.19	0.04
West and North Vancouver Island	2002	0.28	0.69	1.24
West and North Vancouver Island	2003	-0.20	0.16	0.64
West and North Vancouver Island	2004	0.28	0.70	1.27
West and North Vancouver Island	2005	-0.22	0.13	0.65
West and North Vancouver Island	2006	0.10	0.33	0.62
West and North Vancouver Island	2008	-0.28	0.23	0.93
West and North Vancouver Island	2009	-0.26	-0.11	0.08
West and North Vancouver Island	2010	-0.35	0.13	0.82
West and North Vancouver Island	2011	-0.28	0.21	0.91
West and North Vancouver Island	2012	-0.43	0.03	0.70
West and North Vancouver Island	2013	-0.52	-0.05	0.64
West and North Vancouver Island	2016	-0.11	0.15	0.52
Haida Gwaii	2010	-0.12	0.07	0.30
North Mainland Coast	2005	-0.51	-0.41	-0.28
South Mainland Coast	2001	-0.21	-0.06	0.12
South Mainland Coast	2006	0.08	0.28	0.53
South Mainland Coast	2010	0.15	0.35	0.59

[a] Statistical significance is attributed when the 95% credible interval does not overlap with zero.

Test for associations between radar counts and oceanic indices

There were no consistent associations between predicted regional mean counts and mean SST at lags of zero and one year across the different conservation regions. Estimates of age two herring abundance varied widely over the years and across the conservation regions. The relationship between murrelet radar counts and age two herring recruitment was consistently positive for each of the six regions with, for example, R^2 values ranging 1% to 89% (Fig. 3). There were, however, no significant associations between radar count by region and age two herring recruitment (i.e., all slope parameters had $P > 0.05$). Similarly, we found no consistent associations between radar count and age two herring lagged at one and two years (to indicate age zero and age one herring recruitment).

DISCUSSION

Temporal trends in abundance in British Columbia

Using radar count data from 1996 to 2013, Bertram *et al*. (2015) found a negative overall trend of -1.6%/yr (95% credibility interval: -3.2%, 0.01%), which was interpreted as moderate evidence for a coast-wide decline in the abundance of Marbled Murrelets. In this update, we included more recent data to 2018 and found this negative population trajectory continued during the additional five years with a trend of -2.4%/yr, a trend that is statistically significant (Table 3). Like Bertram *et al*. (2015), we found that this trend varied among conservation regions, with significant negative trends at Haida Gwaii, Central Mainland Coast, East Coast Vancouver Island, and South Mainland Coast. The main regional difference in trends between the two analyses occurred at Central Mainland Coast, where the inclusion of more counts from 2017 resulted in a negative trend (-1.4%/yr) that was not observed previously in the Bertram *et al*. (2015) analysis (note: in 2017, only two of 10 long-term monitoring locations were sampled, so the sample size was limited). Furthermore, Bertram *et al*. (2015) documented positive or neutral trends at Western and North Vancouver Island and the Central Mainland Coast, two regions with the largest populations of murrelets. In contrast, this updated trend analysis found that the median regional trend estimates were negative for all six conservation regions (Table 3), indicating that population declines occurred throughout the province and suggesting a common underlying mechanism. Radar counts of murrelets have been repeatedly correlated with the amount of old-growth nesting habitats (Raphael *et al.* 2002, Burger *et al.* 2004), and Long *et al*. (2011) found that the extent of old-growth nesting habitats decreased throughout British Columbia over a 30-year period from 1987 to 2008. We found that the marine parameters we considered had a weak effect on counts of murrelets, a conclusion that is consistent with reports from Raphael *et al.* (2015), who found that murrelet at-sea abundance and distribution along the Pacific Coast, from Washington State to California from 2000 to 2012, was primarily determined by the proximity to terrestrial nesting habitat. Together, these results indicate that temporal trends in murrelet abundance are likely driven largely by the ongoing loss of coastal old-growth forests.

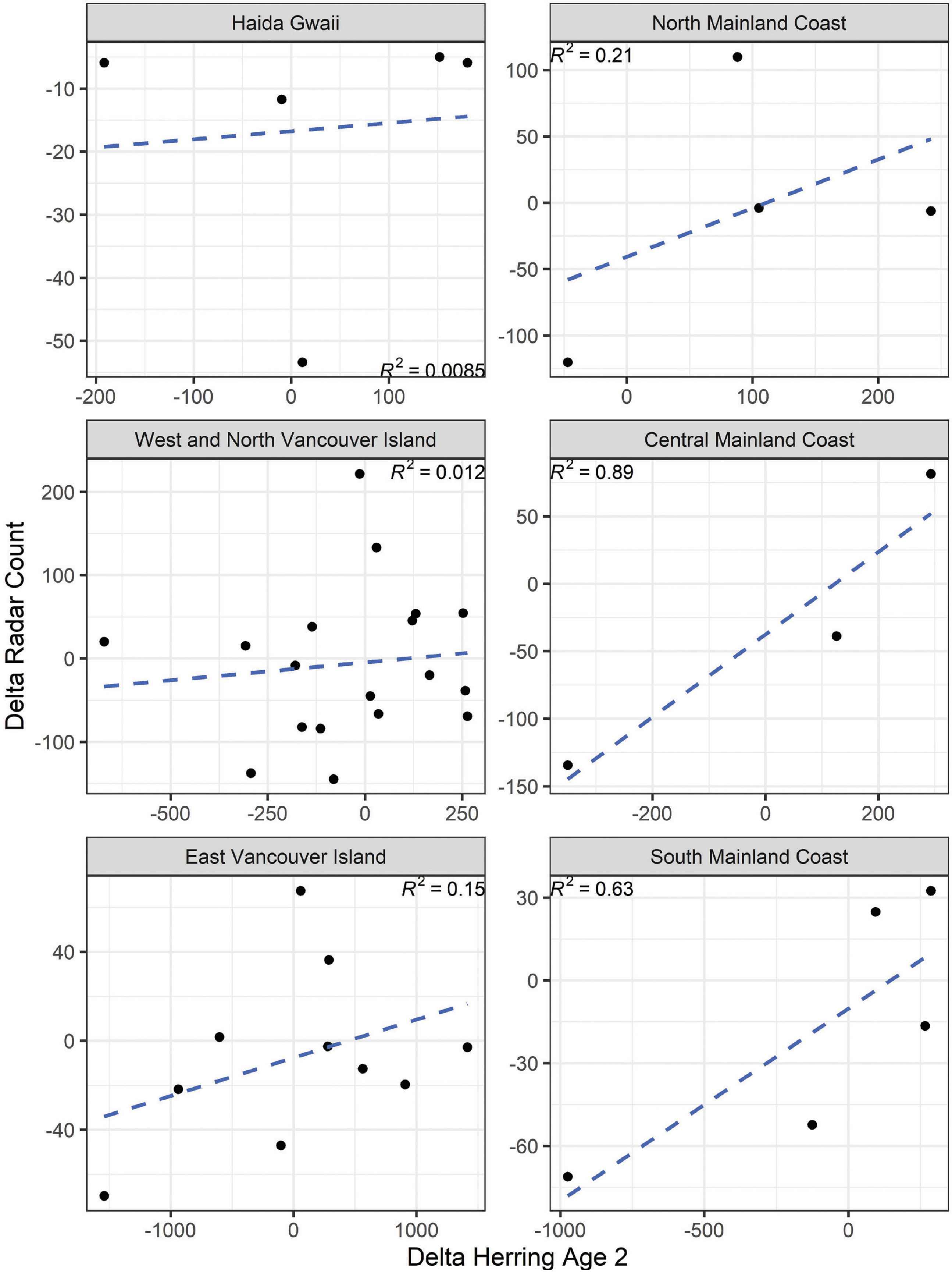

Fig. 3. Association of Marbled Murrelets *Brachyramphus marmoratus* counted at six conservation regions in British Columbia, as predicted with a hierarchical Bayesian model, with measures of abundance of Pacific Herring *Clupea pallasii*. Dashed lines indicate a non-statistically significant fit of a linear model.

Effects of marine conditions

We found that 'The Blob', which was present 2014–2016, did not have a strong effect on Marbled Murrelet abundance. The year effects for 2016 and 2018 were not statistically significant, and we only found weak potential associations between SST and radar counts within each region. We did find relationships between age two herring abundance and counts of murrelets that were consistent among all six conservation regions. These associations (both marine indices and the relationship to murrelet counts) should be further explored with more comprehensive datasets than we had available in this study.

The weak association between SST and radar counts of murrelets contrasts with the mortality events of other marine bird species that occurred during this period (Gibble *et al*. 2018, Jones *et al*. 2018, Drever *et al*. 2018, Piatt *et al*. 2020). Radar counts and counts of carcasses along the shore may not be comparable. Murrelets increase their foraging rates when feeding conditions are poor (Ronconi & Burger 2008); under these conditions, murrelets may conduct more flights between areas, and this increased effort may obscure a decrease in abundance. Alternatively, the effects of the marine heatwave may have been dampened near the coastal areas used by murrelets. Nonetheless, our results are consistent within British Columbia, where only a weak association between murrelet abundance and SST had previously been shown (Burger 1999). Furthermore, the strongest effects from 'The Blob' on basic ocean processes (e.g., upwelling) were felt during the winter (Drever *et al.* 2018), and it may be that differences in conditions during the breeding period, which was considered in this study, were not as distinct from long-term average conditions. Other factors, such as a decrease in food quality, which was found to occurr in Alaska during this heatwave (von Biela *et al.* 2019), was beyond the scope of our study, but such effects remain a research priority. We conclude that the marine heatwave of 2014–2016 did not strongly affect long-term trends in murrelet abundance and that radar counts continue to serve as a useful monitoring tool for Marbled Murrelet abundance in British Columbia.

Improvements in the statistical model

The updated model had substantially better diagnostic outputs compared to the model adopted in Bertram *et al.* (2015) and avoided anomalous parameter estimates by applying important constraints on key model components. Replacing the lognormal likelihood function with a negative binomial likelihood function allowed the zero counts to be retained and did not require their transformation to one's, as was done with the lognormal likelihood function. Year effects were considered to be involved at all sites within a region in the same way. Should sufficient amounts of data become available by site, it may be possible for year effects to be estimated for each site, and it is possible that year effects may be different between sites. In this study, however, given that relatively few observations were available for each year at many of the sites, year effect estimation per site was not feasible. The estimation of station-specific year effects may be desirable to provide greater resolution about the effects of variable ocean conditions relative to long-term changes in nesting habitats. A key step for regions with multiple sites measured in each year (i.e., East Coast Vancouver Island and North and West Vancouver Island) was to identify a reference year in which the year effect could be set to zero within a region. In regions with relatively few years of data, this step involved setting common year effects to zero, where only one or relatively few sites were observed in a given year, which led to relatively few year effects being estimated. This underscores the need to sample multiple sites per year when sampling does occur.

The results reported herein are consistent with the hypothesis that population declines of Marbled Murrelets in British Columbia result from the ongoing loss of coastal old-growth forests that provide nesting habitat for murrelets. Landscapes with more mature forest are most likely to be occupied by murrelets (Betts *et al.* 2020), and therefore, conservation planning for the recovery of Marbled Murrelets will require explicit consideration of how to retain suitable nesting habitat across British Columbia.

ACKNOWLEDGMENTS

We thank the Canadian Marbled Murrelet Recovery Team and collaborations with Peter Arcese that led to the development of a robust monitoring design to detect population trends in Marbled Murrelets within British Columbia. Deborah Faust provided database support. We thank the many field crew members who have conducted radar surveys in British Columbia over the years. Permission to work in Gwaii Haanas National Marine Park Reserve was obtained from Parks Canada and the Archipelago Management Board. Finally, addressing comments of the editors (D. Ainley and R. Johnson) and three anonymous reviewers greatly improved our paper.

REFERENCES

BERTRAM, D.F., DREVER, M.C., MCALLISTER, M., SCHROEDER, B., LINDAY, D. & FAUST, D. 2015. Estimation of coast-wide population trends of Marbled Murrelets in Canada using a Bayesian hierarchical model. *PLoS One* 10: e0134891.

BETTS, M.G., NORTHRUP, J.M., GUERRERO, J.A.B. ET AL. 2020. Squeezed by a habitat split: Warm ocean conditions and old-forest loss interact to reduce long-term occupancy of a threatened seabird. *Conservation Letters* 13: e12745.

BOND, N.A., CRONIN, M.F., FREELAND, H. & MANTUA, N. 2015. Causes and impacts of the 2014 warm anomaly in the NE Pacific. *Geophysical Research Letters* 42: 3414–3420.

BURGER, A.E. 1999. Birds in hot water: responses by Marbled Murrelets to variable ocean temperatures off southwestern Vancouver Island. In: DARLING, L.M. (Ed.) *Proceedings of a Conference on the Biology and Management of Species and Habitats at Risk, Kamloops, BC, 15–19 February 1999*. Victoria, Canada: BC Ministry of Environment, Lands and Parks.

BURGER, A.E., CHATWIN, T.A., CULLEN, S.A., HOLMES, N.P., MANLEY, I.A., MATHER, M.H. ET AL. 2004. Application of radar surveys in the management of nesting habitat of Marbled Murrelets *Brachyramphus marmoratus*. *Marine Ornithology* 32: 1–11.

BURKETT, E.E. 1995. Marbled murrelet food habits and prey ecology. In: RALPH, C.J., HUNT, G.L., RAPHAEL, M.G., PIATT, J.F. (Eds). *Ecology and Conservation of the Marbled Murrelet*. General Technical Report. PSW-GTR-152. Albany, USA: US Department of Agriculture, Forest Service. pp. 223–246.

COSEWIC. 2012. *COSEWIC assessment and status report on the Marbled Murrelet Brachyramphus marmoratus in Canada*. Ottawa, Canada: Committee on the Status of Endangered Wildlife in Canada. [Available online at: www.registrelep-sararegistry.gc.ca/default_e.cfm.]

DI LORENZO, E. & MANTUA, N. 2016. Multi-year persistence of the 2014/15 North Pacific marine heatwave. *Nature Climate Change* 6: 1042–1047.

FRÖLICHER, T.L. & LAUFKÖTTER, C. 2018. Emerging risks from marine heat waves. *Nature Communications* 9: 650.

GIBBLE, C., DUERR, R., BODENSTEIN, B., LINDQUIST, K., LINDSEY, J., BECK, J. ET AL. 2018. Investigation of a large-scale Common Murre (*Uria aalge*) mortality event in California, USA, in 2015. *Journal of Wildlife Diseases* 54: 569–574.

HILBORN, R. & MANGEL, M. 1997. *The Ecological Detective: confronting models with data*. Princeton, USA: Princeton University Press.

JONES, T., DIVINE, L.M., RENNER, H., KNOWLES, S., LEFEBVRE, K.A., BURGESS, H.K. ET AL. 2019. Unusual mortality of Tufted Puffins (*Fratercula cirrhata*) in the eastern Bering Sea. *PLoS One* 14: e0216532.

JONES, T., PARRISH, J.K., PETERSON, W.T., BJORKSTEDT, E.P., BOND, N.A., BALLANCE, L.T. ET AL. 2018. Massive mortality of a planktivorous seabird in response to a marine heatwave. *Geophysical Research Letters* 45: 3193–3202.

LONG J.A., HAZLITT, S.L., NELSON, T.A. & LABEREE, K. 2011. Estimating 30-year change in coastal old-growth habitat for a forest-nesting seabird in British Columbia, Canada. *Endangered Species Research* 14: 49–59.

LORENZ, T.J. & RAPHAEL, M.G. 2018. Declining Marbled Murrelet density, but not productivity, in the San Juan Islands, Washington, USA. *The Condor: Ornithological Applications* 120: 201–222.

MANLEY, I.A. 2006. *Inventory methods for Marbled Murrelet radar surveys. Standards for Components of British Columbia's Biodiversity No. 1a*. Victoria, Canada: Resources Information Standards Committee, Ecosystems Branch, British Columbia Ministry of Environment. [Available online at: http://ilmbwww.gov.bc.ca/risc/index.htm.]

MCALLISTER, M.K. 2019. *Updated analysis of trends in radar counts of Marbled Murrelets in British Columbia*. Unpublished contract report. Delta, Canada: Environment and Climate Change Canada.

MCFARLANE-TRANQUILLA, L.M., PARKER, N.R., BRADLEY, R.W., LANK, D.B., KREBS, E.A. ET AL. 2005. Breeding chronology of Marbled Murrelets varies between coastal and inshore sites in southern British Columbia. *Journal of Field Ornithology* 76: 357–367.

McIVER, W., BALDWIN, J., LANCE, M.M., PEARSON, S.F., STRONG, C., LYNCH, D. ET AL. 2019. *Marbled murrelet effectiveness monitoring, Northwest Forest Plan: At-sea Monitoring, 2019 Summary Report*. Portland, USA: Northwest Forest Plan Interagency Regional Monitoring Program.

OLIVER, E.C., DONAT, M.G., BURROWS, M.T., MOORE, P.J., SMALE, D.A., ALEXANDER, L.V., ET AL. 2018. Longer and more frequent marine heatwaves over the past century. *Nature Communications* 9: 1–12.

PIATT, J.F., PARRISH, J.K., RENNER, H.M., SCHOEN, S.K., JONES, T.T., ARIMITSU, M.L. ET AL. 2020. Extreme mortality and reproductive failure of Common Murres resulting from the northeast Pacific marine heatwave of 2014-2016. *PLoS One* 15: e0226087.

RAPHAEL, M.G., EVANS MACK, D. & COOPER, B.A. 2002. Landscape-scale relationships between abundance of Marbled Murrelets and distribution of nesting habitat. *The Condor* 104: 331–342.

RAPHAEL, M.G., SHIRK, A.J., FALXA, G.A. & PEARSON, S. F. 2015. Habitat associations of marbled murrelets during the nesting season in nearshore waters along the Washington to California coast. *Journal of Marine Systems* 146: 17–25.

RONCONI, R.A. & BURGER, A.E. 2008. Limited foraging flexibility: increased foraging effort by a marine predator does not buffer against scarce prey. *Marine Ecology Progress Series* 366: 245–258.

SPIEGELHALTER D. J., BEST, N.G., CARLIN, B.P. & VAN DER LINDE A. 2002. Bayesian measures of model complexity and fit. *Journal of the Royal Statistical Society: Series B (Statistical Methodology)* 64: 583–640.

VON BIELA, V.R., ARIMITSU, M.L., PIATT, J.F., HEFLIN, B., SCHOEN, S.K., TROWBRIDGE, J.L. ET AL. 2019. Extreme reduction in nutritional value of a key forage fish during the Pacific marine heatwave of 2014–2016. *Marine Ecology Progress Series* 613: 171–182.